Adaptive Integral Sliding Mode Controller for Longitudinal Rotation Control of a Tilt-Rotor Aircraft

Jin H. Kim[1], S. Andrew Gadsden[1] and Stephen A. Wilkerson[2]

Abstract— **This paper presents an adaptive integral sliding mode controller for longitudinal rotation control of a tilt-rotor aircraft (TRA). The movable mass, which slides along the wing of the TRA, is considered an unknown disturbance in this paper. The simplified dynamics of the TRA is proposed for the control of the longitudinal rotation during its landing, and application of the adaptive integral sliding mode controller is presented. In the design process of the controller, we applied a sliding surface including an integral term for reinforcing the control performance of the system. This paper compares the results of applying a PID controller and the adaptive integral sliding mode controller with the proposed sliding surface for improved robustness and stability to unknown disturbance.**

Fig. 1. A tiltrotor aircraft, V-22 Osprey [16].

I. INTRODUCTION

Vertical take-off and landing (VTOL) aircraft have been used in various fields for both military and civilian applications, including reconnaissance, transportation, rescue, and recovery. A tilt-rotor aircraft (TRA), a type of VTOL aircraft, is actively utilized. The main characteristic of the TRA is that it generates lift and propulsion by rotors mounted on rotating engines at the ends of a fixed wing. This main characteristic leads the TRA to have advantages over both helicopters and fixed-wing aircraft because, not only can the TRA achieve long flight distances with relatively high speeds, it can also take-off and land vertically. However, one disadvantage is highly coupled nonlinearities, which causes degradation in stability. Hence, to solve this problem, various nonlinear control techniques have been applied and researched [1], [2]. Tilt-rotor unmanned aerial vehicles (TRUAVs) bave been developed further as per [3]-[6].

R. T. Rysdyk *et al*. presented nonlinear adaptive flight control techniques using artificial neural networks (ANNs) for the TRA in [1] and [2]. In addition, ANNs were applied to the model inversion control technique for overcoming the drawback of dynamic model inversion control; however, this process is sensitive to modeling errors. The proposed control architecture minimized the requirement of the conventional control method which is extensive gain scheduling, and also adapted well to uncertainties in the control inputs and state variables.

A controller based on back-stepping was presented for an autonomous flight of the TRUAV by F. Kendoul *et al*. [3]. The proposed TRUAV model allowed the rotors to tilt in not only the lateral axis, but also the longitudinal axis of the rotor. The tilting of the rotor yielded an increase in the pitch stability. Furthermore, this paper applied the back-stepping strategy for the controller.

In [4], an autopilot design of the TRUAV was presented using particle swarm optimization methods. The proposed control technique solved problems that are caused by various dynamic characteristics and system nonlinearities. This control design achieved the required stability margin in every flight mode that was tested.

A dynamic model and nonlinear control scheme was presented for autonomous TRUAV hovering in [5]. The controller was designed from decoupled dynamics and was based on Lyapunov stability theory and considered a bounded, smooth function. TRUAV model and attitude control was presented by C. Papachristors *et al*. [6]. For attitude control, a PID controller was applied to the system with a simple model obtained through first-order linearization.

For the control of nonlinear TRUAV system, various controllers have been introduced [1]-[6]. In this paper, we consider a sliding mode controller (SMC) which is a nonlinear and robust controller. It attempts to change the control signal in order for the system to reach a stable origin in an exponential fashion, despite the existence of bounded uncertainties such as external disturbances, modeling errors, and sensor noise [7]-[8]. For these advantages, SMC has been applied to various robotic systems, such as robotic manipulators and ground/aerial vehicles [9]-[15]. Applications of

[1]Jin H. Kim and S. Andrew Gadsden are with the Department of Mechanical Engineering, University of Maryland, Baltimore County, 1000 Hilltop Circle, Baltimore, MD 21250, USA, umbcjhkim@umbc.edu, gadsden@umbc.edu

[2]Stephen A. Wilkerson is with the Department of Engineering and Computer Science, York College, York, PA 17403, USA, swilkerson@ycp.edu

SMCs on quadrotors are presented in [11]-[13].

Furthermore, we also consider sliding surface with an integral term, which is proposed for improved control performance. This is called as an integral SMC, and was proposed in [17]. The integral SMC guarantees robustness through an entire response of the system starting from the initial time instance. Because the order of the motion equation in integral sliding mode is equal to the order of the original system.

In this paper, the longitudinal control of a TRA with an unknown disturbance is considered. To control the roll angle during landing with an unknown disturbance caused by a movable mass, we propose an adaptive integral SMC for the TRA, derived by Lyapunov stability theory with an integral term in a sliding surface.

The rest of the paper is organized as follows. Section II introduces the TRA system model and the simplified longitudinal dynamics with an unknown disturbance. Section III describes the sliding surface with the integral term, and the adaptive integral sliding mode controller for the TRA with unknown disturbances. In Section IV, the simulation results of the proposed controller are presented and compared with the PID controller. Section V presents concluding remarks and future experimental work.

II. DYNAMIC MODEL

The dynamics of the TRA for designing the controller are introduced in this section. The TRA, which has two tilt-able rotors fixed on a rigid wing frame, is considered as shown in Fig. 2. In this paper, the dynamics are simplified such that the rotors are able to rotate around the lateral axis only, and the flight control surfaces of the fixed-wing aircraft are not considered. Future work will study these additional effects.

A. Full Dynamics

Consider the fixed inertia frame I, body frame B and each rotor frame I_n ($n=1,2$), as shown in Fig. 2. The I is defined by axes I_x, I_y and I_z.

The coordinates of the TRA are defined as $x = [x,y,z,\phi,\theta,\psi] \in \mathbb{R}^6$ where $\xi = (x,y,z) \in \mathbb{R}^3$ represents the position of the center of the mass and $\eta = (\phi,\theta,\psi) \in \mathbb{R}^3$ represents the roll, pitch, and yaw angle, respectively.

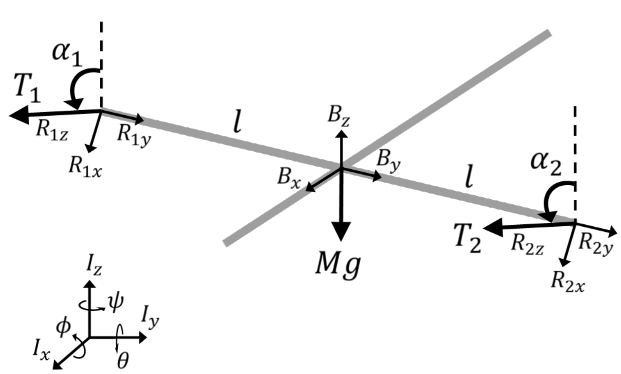

Fig. 2. A tiltrotor aircraft coordinate system.

The B is located at the center of mass and the R_n is attached to the end of the wing. The distance between $textitB$ and R_n is denoted by l, half the length of the wing span.

The rotation of the body in the inertia frame can be given by rotational matrix R_0 using Z-Y-X Euler angles,

$$R_0 = \begin{bmatrix} c\theta c\psi & s\phi s\theta c\psi - c\phi s\psi & c\phi s\theta c\psi + s\phi s\psi \\ c\theta s\psi & s\phi s\theta s\psi + c\phi c\psi & c\phi s\theta s\psi - s\phi c\psi \\ -s\theta & s\phi c\theta & c\phi c\theta \end{bmatrix}, \quad (1)$$

where c and s denote cosine and sine functions, respectively. Also, the rotational matrices of the rotors in the body frame are presented as

$$R_n = \begin{bmatrix} c\alpha_n & 0 & s\alpha_n \\ 0 & 1 & 0 \\ s\alpha_n & 0 & c\alpha_n \end{bmatrix}, \quad (2)$$

where α_n denotes tilt angles of rotors around R_{ny}.

The dynamic equations of the TRA model can be derived from an Newton-Euler approach, and is simplified as follows:

$$\begin{aligned} \dot{\xi} &= v \\ \dot{v} &= \frac{1}{M}(\sum_{n=1}^{2} T_n R_0 R_n \bar{e}_3) - g\bar{e}_3 \\ \dot{R_0} &= R_0\dot{\omega} \\ J_b\dot{\omega} &= -\omega \times J_b\omega - \sum_{n=1}^{2} J_r(\omega \times \bar{e}_3)\Omega_n + \tau_a, \end{aligned} \quad (3)$$

where Ω_n denotes the speed of each rotor, T_n is the thrust of each rotor. $[J_b, J_r]$ presents body and rotor inertia, respectively. $e_3 = [0,0,1]^T$, and τ_a denotes the torque on the body of the TRA, M is the mass of the TRA, and g denotes gravity. The rotational matrices R_0 and R_n can be simplified as one rotational matrix, $R_{0,n}$, then the second dynamic equation of (3) can be rewritten as follows:

$$\dot{v} = \frac{1}{M}(\sum_{n=1}^{2} T_n R_{0,n}\bar{e}_3) - g\bar{e}_3. \quad (4)$$

Since TRA uses the same tilting angles in practice, assume that α_1 is equal to α_2. Therefore, the forces, F_a, and torques, τ_a, applied on the body of the TRA can be written as (5) and (6), respectively. This yields:

$$\begin{aligned} F_a &= T_1 R_{0,1}\bar{e}_3 + T_2 R_{0,2}\bar{e}_3 - g\bar{e}_3 \\ &= (T_1+T_2)R_{0,1}\bar{e}_3 - g\bar{e}_3 \\ &= (T_1+T_2)\begin{bmatrix} c\theta c\psi s\alpha_1 + c\phi s\theta c\psi c\alpha_1 + s\phi s\psi c\alpha_1 \\ c\theta s\psi s\alpha_1 + +c\phi s\theta s\psi c\alpha_1 - s\phi c\psi c\alpha_1 \\ c\phi c\theta c\alpha_1 - s\theta s\alpha_1 - g/(T_1+T_2) \end{bmatrix}, \end{aligned} \quad (5)$$

$$\begin{aligned} \tau_a &= \begin{bmatrix} l(T_2 c\alpha_2 - T_1 c\alpha_1) \\ 0 \\ l(T_1 s\alpha_1 - T_2 s\alpha_2) \end{bmatrix} \\ &= \begin{bmatrix} l(T_2 - T_1)c\alpha_1 \\ 0 \\ l(T_1 - T_2)s\alpha_1 \end{bmatrix}. \end{aligned} \quad (6)$$

Hence, the full dynamics of the TRA can be rewritten with defined input terms (7), as shown in (8)-(13).

$$u_1 = T_1 + T_2$$
$$u_2 = \frac{l(T_1 - T_2)}{J_b} \tag{7}$$

$$\ddot{x} = u_1(cos\psi sin\alpha_1 + sin\phi sin\psi cos\alpha_1) \tag{8}$$

$$\ddot{y} = u_1(sin\psi sin\alpha_1 - sin\phi cos\psi cos\alpha_1) \tag{9}$$

$$\ddot{z} = u_1 cos\phi cos\alpha_1 - g \tag{10}$$

$$\ddot{\phi} = -u_2 cos\alpha_1 \tag{11}$$

$$\ddot{\theta} = 0 \tag{12}$$

$$\ddot{\psi} = u_2 sin\alpha_1. \tag{13}$$

Note again that these dynamics are derived without consideration of the wing control surfaces; with fixed-pitch tilt rotors only. Hence, (12) is not controllable in this setup. This indicates that θ does not affect any state variables, and we assume the initial θ is zero so that we can derive the full dynamics of the TRA with this assumption. Furthermore, to solve the problem proposed in this paper, it is assumed that the TRA is controlled with an α_n of zero degrees during landing.

B. Longitudinal Dynamics with an Unknown Disturbance

In this paper, longitudinal rotation control of a TRA is considered with an unknown disturbance caused by a movable mass during its landing. Assume that there is a movable mass that translates along the longitudinal axis. One can extract and simplify ϕ dynamics adding the unknown disturbance term as represented in (14), and a shown in Fig. 3. l_m is the distance between the center of the mass of the system and the position of the movable mass.

$$\ddot{\phi} = \frac{l}{J_x}(T_2 cos\alpha_2 - T_1 cos\alpha_1) + f_r(\phi), \tag{14}$$

where the term $f_r(\phi)$ is an unknown disturbance due to a movable mass.

Next, define a control input term (15) with the same tilt angles α_1 and α_2 assumed above. The final simplified equation of motion can be rewritten as (16).

$$u = \frac{(T_2 - T_1)cos\alpha_1}{J_x} \tag{15}$$

$$\ddot{\phi} = lu + f_r(\phi). \tag{16}$$

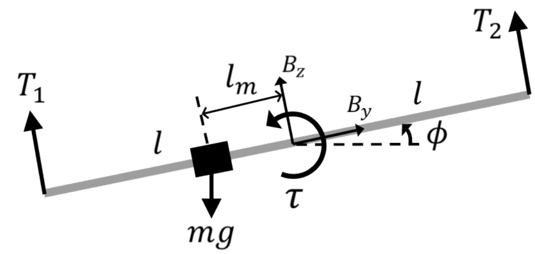

Fig. 3. A tiltrotor aircraft coordinate system.

III. ADAPTIVE INTEGRAL SLIDING MODE CONTROLLER

In order to overcome the unknown disturbance, an adaptive integral sliding mode controller is presented in this section. This strategy is based on [17]. In order to improve the control performance, an integral sliding surface is used instead of a PD-type sliding surface. The addition of the I helps reduce steady-state error.

First, we define the suitable sliding surface, s. The general sliding surface is defined as

$$s(t) = \dot{e}(t) + ke(t), \tag{17}$$

where k is a positive constant and $e(t) = \phi(t) - \phi_d(t)$, in which ϕ_d denotes the desired state variable.

Consider an integral term such that the new sliding surface can be written as per (18).

$$s(t) = k_1 e(t) + \dot{e}(t) + k_2 \int_0^t e(\tau)d\tau - \dot{e}(0) - k_1 e(0), \tag{18}$$

where k_1 and k_2 denotes the controller parameters.

According to SMC theory, the sliding surface should equal zero with the designed controller input, making the trajectory of the system stay on s [7]. In order to accomplish this task, a Lyapunov function is selected as [14]

$$L = \frac{1}{2}s^T s + \frac{1}{2}\tilde{f}_r^T \tilde{f}_r, \tag{19}$$

where $\hat{f}_r(\phi)$ denotes the estimated value of $f_r(\phi)$, and $\tilde{f}_r(\phi)$ is the definition of the error between the true and estimated values, that is, $\tilde{f}_r(\phi) := f_r(\phi) - \hat{f}_r(\phi)$. From the above function, the time derivative of the Lyapunov function can be defined as follows:

$$\begin{aligned}\dot{L} &= s\dot{s} + \tilde{f}_r\dot{\tilde{f}}_r \\ &= s(k_1\dot{e} + \ddot{e} + k_2 e) + \tilde{f}_r(\dot{f}_r - \dot{\hat{f}}_r) \\ &\leq 0.\end{aligned} \tag{20}$$

Here, assume that the mass on the system moves slowly due to surface friction resulting in a slow change of $f_r(\phi)$, thereby assuming that $\dot{f}_r \approx 0$. That is, $\dot{\tilde{f}}_r(\phi) \approx -\dot{\hat{f}}_r(\phi)$. Then, (20) can be rewritten as

$$\begin{aligned}\dot{L} &= s(k_1\dot{e} + \ddot{e} + k_2 e) + \tilde{f}_r(\phi)(-\dot{\hat{f}}_r(\phi)) \\ &= s\{k_2 e + lu + f_r(\phi) - \ddot{\phi}_d + k_1\dot{e}\} - \tilde{f}_r(\phi)\dot{\hat{f}}_r(\phi) \\ &\leq 0.\end{aligned} \tag{21}$$

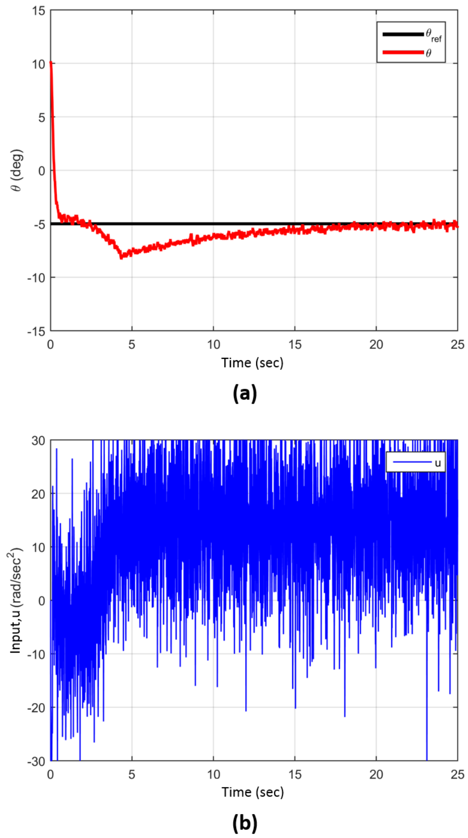

Fig. 4. PID controller results (Case 1). (a) The history of θ, (b) the history of u.

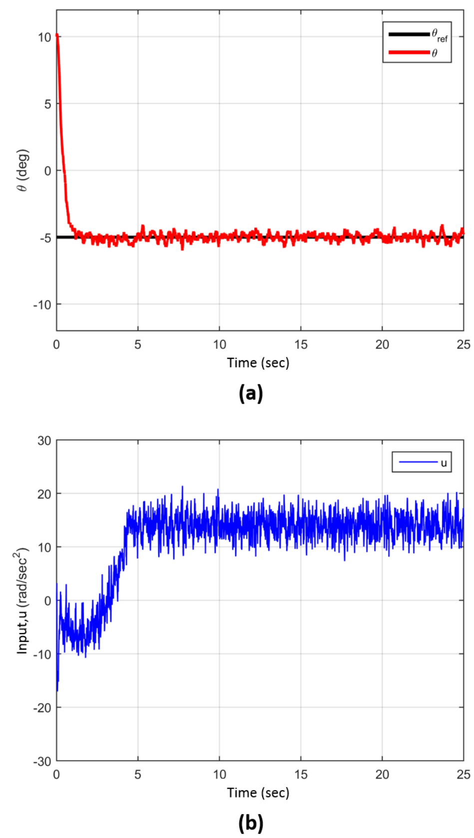

Fig. 5. Results of the proposed controller (Case 1). (a) The history of θ, (b) the history of u.

To guarantee the stability of system equilibrium, (21) must be negative semi-definite as per Lyapunov theory [8]. Hence, the input term u is defined as

$$u = \frac{1}{l}\{-k_2 e - \hat{f}_r(\phi) + \ddot{\phi}_d - k_1\dot{e} - Csgn(s)\}, \tag{22}$$

where C is a positive input gain. Then (21) becomes

$$\dot{L} = \tilde{f}_r(\phi)(s - \dot{\hat{f}}_r(\phi)) - Cs^2 \leq 0. \tag{23}$$

When $\dot{\hat{f}}_r(\phi)$ is updated as $k_1 e(t) + \dot{e}(t) + k_2 \int_0^t e(\tau)d\tau - \dot{e}(0) - k_1 e(0)$, the time derivative of Lyapunov function is reduced to

$$\dot{L} = -Cs^2 \leq 0. \tag{24}$$

Therefore, the system can reach the sliding surface ($s = 0$) in a finite period of time with the control input (22).

In order to avoid the effects of chattering caused by the switching term in the control input, a saturation function is implemented, as shown in (25); instead of $sgn(s)$ in this paper.

$$sat(s(t), \Gamma) = \begin{cases} \frac{s(t)}{\Gamma} & \text{if } |s(t)| < \Gamma \\ sgn(s(t)) & \text{otherwise} \end{cases}, \tag{25}$$

where Γ is the boundary layer of saturation function (user defined parameter).

IV. SIMULATION

In this section, the proposed controller is applied and simulated on the TRUAV system. Two cases were simulated for controlling ϕ. The first case considers constant reference signals, and the second case considers a cosine function reference. To compare the performance of the proposed controller, a PID controller was tested under the same conditions. The results illustrate the state variable changes, control input, and error with sensor noise. In this simulation, sensor noise was used with a mean and standard deviation of 0 deg and 0.115 deg, respectively. The physical limitation of the output was set at $\pm 30\ rad/sec^2$. Relevant simulation parameters are defined as follows:

$$\begin{aligned} & l = 0.5\ m,\ l_{m,init} = -0.1\ m \\ & m = 3\ kg,\ g = 9.81\ m/s^2 \\ & \phi_{init} = 10\ deg \\ & J_b = 1.25\ Ns^2/rad \\ & k_P = 250,\ k_I = 50,\ k_D = 140 \\ & k_1 = 15,\ k_2 = 40,\ C = 15 \\ & \Gamma = 0.5 \end{aligned} \tag{26}$$

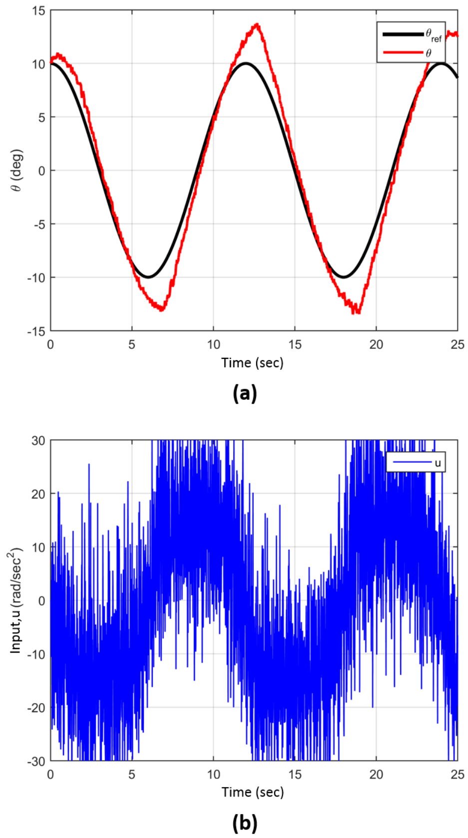

Fig. 6. PID controller results (Case 2). (a) The history of θ, (b) the history of u.

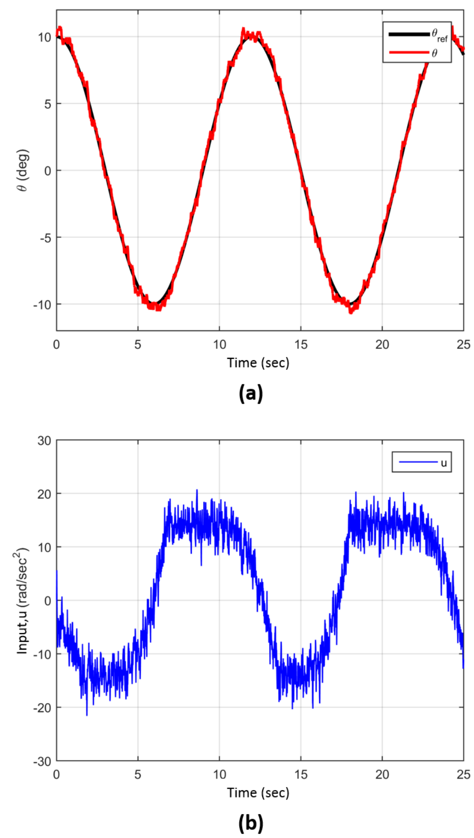

Fig. 7. The results of the proposed controller. (Case 2) (a) : The history of θ, (b) : the history of u.

We assume that ϕ affects the movement of the mass, loaded in the TRA. Hence, the location of the movable mass can be written as shown in (27).

$$l_m(t) = l_{m,init} + \int_0^t \int_0^t \left(gsin\left(\phi(\tau)\right) - \mu gcos\left(\phi(\tau)\right)\right) d\tau d\tau, \tag{27}$$

where $l_{m,init}$ denotes the initial distance between the conter of the mass of the system and the position of the movable mass, and μ is a friction coefficient. From (27), we can write $f_r(\phi)$ in the logitudinal dynamics of a TRA as (28).

$$f_r(\phi(t)) = \frac{l_m(t)}{J_m} mgcos\left(\phi(t)\right), \tag{28}$$

where J_m represents mass inertia. Note that the estimation of an unknown disturbance, $\hat{f}_r(\phi(t))$, is updated from $\dot{\hat{f}}_r(\phi) = k_1 e(t) + \dot{e}(t) + k_2 \int_0^t e(\tau)d\tau - \dot{e}(0) - k_1 e(0)$ for the proposed controller.

A. Case 1

In this case, the reference input is set to -5 deg, the initial position of the mass $l_{m,init}$ is -0.1 m, and the initial roll angle ϕ_{init} is -10 deg, which is off the initial reference input. The results of this case are shown in Figs. 4 and 5. Both controllers performed well and generated acceptable outputs. However, as per Fig. 4(a), the PID controller demonstrated overshoot of about 60% at about 3-5 seconds. This is due to the fact that the PID controller does not accurately respond to the effect of the movable mass. The additional control action is required in order to stay within a region of the reference trajectory until the mass stops moving. However, the proposed integral sliding mode controller was able to overcome the effects of the unknown disturbance, and generated a suitable control input at each moment as shown in Fig. 5. The results of this simulation show better tracking performance when compared with the PID controller. Furthermore, trends of the control inputs illustrate that the PID controller generated large input values, thus requiring more energy; whereas the proposed integral sliding mode controller had smaller input values.

B. Case 2

In the second case, similar initial parameters were used, however the reference input was in the shape of a cosine function. As illustrated in Fig. 6, the results obtained by the PID controller yielded overshoot of about 35% when tracking the reference values. The unwanted overshoot was caused by the moving mass which interjects an unknown disturbance into the control system. In contrast, the proposed integral sliding mode controller operated successfully despite the unknown perturbation as shown in Fig. 7. In Fig. 6(b)

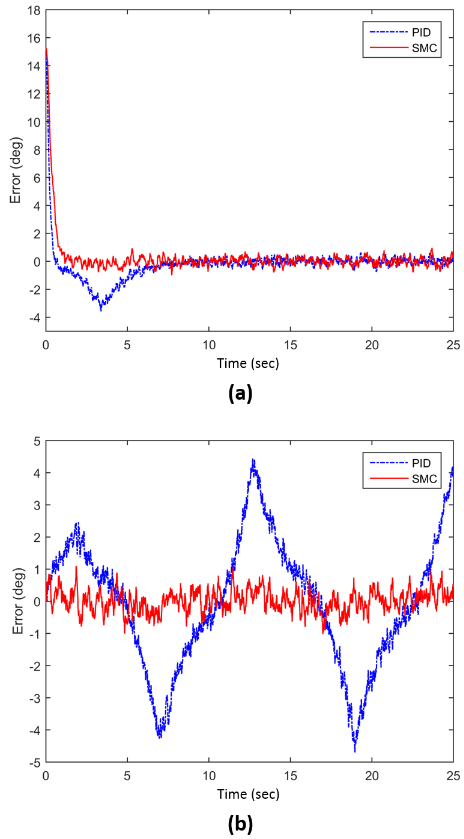

Fig. 8. The histories of errors ($e_\phi = \phi - \phi_d$). (a) The blue dashed line and the red solid line represent e_ϕ from the PID controller and from the proposed controller, respectively, in the first case. (b) The same data in the second case.

and Fig. 7(b), the control inputs are depicted. The proposed controller generated a more efficient and smaller control input signal than the PID controller in this case as well.

C. RMSE

The error values from all of the simulations are depicted in Fig. 8. The root-mean-square errors (RMSE) of each result are calculated as shown in Table I. Note that the units are in degrees. From these results, it is demonstrated that the proposed controller yielded better tracking accuracy when compared with the PID controller, in both cases.

TABLE I

RMSE OF EACH SIMULATION

	Case 1	Case 2
PID controller	0.0332	0.0207
Proposed SMC	0.0230	0.0048

V. CONCLUSIONS AND FUTURE WORK

This paper proposed an adaptive integral sliding mode controller for the control of tilt-rotor unmanned aerial vehicle longitudinal rotation. The simplified longitudinal rotation dynamics was proposed with an unknown disturbance caused by a movable system mass. The proposed controller was applied to the system. In the sliding surface, the integral term was added for improvement of the control performance, whereas a general sliding surface is considered a proportional-derivative-type. Simulation results demonstrate that the proposed controller yields good tracking performance, and is more robust and faster than the PID controller. Future studies will look at implementing the control methodologies in the laboratory environment. Furthermore, this paper will be expanded significantly to include full control of TRUAVs with various nonlinear control strategies under multiple scenarios.

REFERENCES

[1] A. J. Calise, and R. T. Rysdyk, “Nonlinear adaptive flight control using neural networks,” *IEEE Trans. on Control Systems*, vol. 18, no. 6, pp. 14-25, 1998.

[2] R. T. Rysdyk, and A. J. Calise, “Adaptive model inversion flight control for tilt-rotor aircraft,” *Journal of Guidance, Control, and Dynamics*, vol. 22, no. 3, pp. 402-407, 1999.

[3] F. Kendoul, I. Fantoni, and R. Lozano, “Modeling and control of a small autonomous aircraft having two tilting rotors,” *Proc. of the IEEE Conference on Decision and Control the European Control Conference*, Seville, Spain, December 12-15, 2005.

[4] J. Lee, B. Min, and E. Kim, “Autopilot design of tilt-rotor UAV using particle swarm optimization method,” *Proc. of the 44th IEEE International Conference on Control, Automation and Systems*, Seoul, Korea, October 17-20, 2007.

[5] A. Sanchez, J. Escareno, O. Garcia, and R. Lozano, “Autonomous hovering of a noncyclic tiltrotor UAV: Modeling, control and implementation,” *Proc. of the 17th World Congress The International Federation of Automatic Control*, Seoul, Korea, July 6-11, 2008.

[6] C. Papachristos, K. Alexis, and A. Tzes. “Design and experimental attitude control of an unmanned tilt-rotor aerial vehicle,” *Proc. of the 15th IEEE International Conference on AdvancedRobotics*, Tallinn, Estonia, June 20-23, 2011.

[7] V. Utkin, *Sliding Modes in Control Optimization*, New York: Springer-Verlag, 1992.

[8] H. K. Khalil, *Nonlinear Systems*, Prentice Hall, 2002.

[9] Q.P. Ha, D.C. Rye, H.F. Durrant-Whyte, “Fuzzy moving sliding mode control with application to robotic manipulators,” *IEEE Trans. on Automatica*, vol. 35, no. 4, pp. 607-616, 1999.

[10] J.M. Yang and J.H. Kim, “Sliding mode control for trajectory tracking of nonholonomic wheeled mobile robots,” *IEEE Trans. on Robotics and Automation*, vol. 15, no. 3, pp. 578-587, 1999.

[11] S. Bouabdallah, and R. Siegwart, “Backstepping and sliding-mode techniques applied to an indoor micro quadrotor,” *Proc. of the 2005 IEEE International Conference on Robotics and Automation*, Barcelona, Spain, April 18-22, 2005.

[12] H. Xu, M. D. Mirmirani, and P. A. Ioannou, “Adaptive Sliding Mode Control Design for a Hypersonic Flight Vehicle,” *AIAA Trans. on Journal of Guidance, Control, and Dynamics*, vol. 27, no. 5, pp. 829-838, 2006.

[13] R. Xu, and . zgner. “Sliding mode control of a quadrotor helicopter,” *Proc. of the 45th IEEE Conference on Decision and Control*, San Diego, CA, USA, December 13-15, 2006.

[14] D. Lee, H. J. Kim, and S. Sastry, “Feedback linearization vs. adaptive sliding mode control for a quadrotor helicopter,” *IEEE Trans. on International Journal of Control, Automation, and Systems*, vol. 7, no. 3, pp. 419-428, 2009.

[15] V. Jouppila, S. A. Gadsden, S. R. Habibi, G. M. Bone, and A. Ellman, “Sliding mode controller and filter applied to a pneumatic McKibben muscle actuator,” *Proc. of ASME International Mechanical Engineering Congress and Exposition*, Lake Buena Vista, Florida, USA, November 1319, 2009.

[16] V-22 Osprey, http://www.boeing.com/defense/v-22-osprey/

[17] V. Utkin and J. Shi, “Integral sliding mode in systems operating under uncertainty conditions,” *Proc. of the 32th Conference on Decision and Control*, Kobe, Japan, December 11-13, 1996.